SUPPLEMENTARY FILE

TITLE: Outcomes on anti-VEGFR-2/paclitaxel treatment following progression on immune checkpoint inhibition in patients with metastatic gastroesophageal adenocarcinoma.

AUTHORS: Lionel A. Kankeu Fonkoua MD, Sakti Chakrabarti MD, Mohamad B. Sonbol MD, Pashtoon M. Kasi MD MS, Jason S. Starr DO, Alex J. Liu MD, Wendy K. Nevala MS, Rachel L. Maus PhD, Melanie C Bois MD, Henry C. Pitot MD, Chandrikha Chandrasekharan MD, Helen J. Ross MD, Tsung-Teh Wu MD PhD, Rondell P. Graham MBBS, Jose C. Villasboas MD, Matthias Weiss MD, Nathan R. Foster MS, Svetomir N. Markovic MD PhD, Haidong Dong MD PhD, and Harry H. Yoon MD MHS

TABLE OF CONTENTS

MATERIALS & METHODS

Patients and treatment

At our institution a durable clinical response to ramucirumab/paclitaxel was unexpectedly observed in in 2 (of 2) subjects with advanced measurable gastric/GEJ adenocarcinoma who had progressed after pembrolizumab on KEYNOTE-059. Due to the lack of effective salvage treatment options in this disease, interested clinicians in our group decided to adjust clinical practice to treat patients with ramucirumab/paclitaxel over other standard chemotherapy regimens after irRECIST-defined progression on PD-1 blockade. PD-1 blockade was given at physician discretion based on FDA-approved indication, patient assistance, or clinical trial. After approximately one year, we searched our database to identify all patients at Mayo Clinic (Rochester, MN; Jacksonville, FL; and Phoenix, AZ) with advanced gastric/GEJ adenocarcinoma who had received at least one dose of ramucirumab/paclitaxel (1-Jan-2014 to 1-Apr-2019) following at least one dose of anti-PD-1-containing therapy (data cutoff 20-Sept-2019). Initial treatment with ramucirumab + paclitaxel was administered as follows: ramucirumab 8 mg/kg intravenously on days 1 and 15, and paclitaxel 80 mg/m² intravenously on days 1, 8, and 15 of a 28-day cycle.

The Mayo Clinic Unified Data Platform Advanced Cohort Explorer (ACE) query tool and pharmacy administration databases were utilized to identify all patients who received concurrent ramucirumab + paclitaxel. The ACE tool searches for terms and phrases within textual documents including outpatient/inpatient clinical notes and pathology and genetic results, as well as data on diagnosis codes (International Classification of Disease [ICD]-9, ICD-10, Hospital International Classification of Diseases Adapted [HICDA], Current Procedural Terminology

[CPT]) and demographics. Textual documents were searched in ACE using conjunction and disjunction combinations using different terms as below:

- ***Disease search terms***
    - Gastric cancer or carcinoma or neoplasm or adenocarcinoma
    - Stomach cancer or carcinoma or neoplasm or adenocarcinoma
    - (Cancer or carcinoma or neoplasm or adenocarcinoma) of the stomach
    - Malignant Neoplasm Of Stomach, esophagus, GEJ, Gastroesophageal junction, GE junction
    - GEJ or Gastroesophageal junction or GE junction or cancer
    - GEJ or Gastroesophageal junction or GE junction or carcinoma
    - GEJ or Gastroesophageal junction or GE junction or adenocarcinoma
    - GEJ or Gastroesophageal junction or GE junction or neoplasm
    - Esophageal cancer or carcinoma or neoplasm or adenocarcinoma
    - (Cancer or carcinoma or neoplasm or adenocarcinoma) of the esophagus

- ***Search terms for index therapy***
    - Ramucirumab or Paclitaxel or Taxol or RAMTAX
- ***Dates***
    - Index therapy initiated on or after 1/1/2014 and prior to 4/1/2019.

All "hits" resulting from search results were confirmed by chart review of each individual patient. Medical records were reviewed retrospectively and data on clinicopathologic, survival, and treatment related variables were collected using standardized intake forms. No exclusions

of patients were made with regard to PD-L1, HER2, or MMR status, prior response to PD-1 blockade, tumor volume, presence of brain metastases, number of prior lines of therapy, performance status, or other patient-/tumor-related factors. The data cutoff date was 9/20/2019. Study data were collected and managed using REDCap (Research Electronic Data Capture) electronic data capture tools hosted at Mayo Clinic.

Immunofluorescent staining

Tissues were routinely processed and embedded in paraffin in the Mayo Clinic Department of Laboratory Medicine and Pathology. From formalin-fixed paraffin-embedded (FFPE) tissue blocks, 5-micron-thick tumor tissue sections were obtained and stained with hematoxylin and eosin (H&E). H&E slides were reviewed by anatomic pathologists (T-T.W., M.B., R.G) to confirm the presence and enrichment of tumor tissue in the sections.

Tumor-infiltrating immune cells were analyzed using multiplexed immunofluorescence. FFPE tissue sections were stained with two antibody-fluorophore conjugates followed by automated image acquisition, fluorophore inactivation and re-staining in a cyclical manner, resulting in a composite image measuring expression of multiple biomarkers simultaneously at the single-cell level, as previously described.[1]

Antibody purification, conjugation and selection

Antibody purification, conjugation, screening, selection and validation processes were performed as previously published.[1] Commercially available antibodies were purified from bovine serum albumin (BSA), glycerol, or other stabilizing agents by protein A/G purification before

conjugation. Affinity chromatography was used to remove impurities from the vendor antibody to enable conjugation. Protein A (HiTrap Protein A HP Column, GEHC, 17-0402-01) for rabbit antibodies or protein G (HiTrap Protein G HP Column, GEHC, 17-0404-01) for mouse antibodies were used.

After purification, each antibody was conjugated with either cyanine 3 (Cy3) or cyanine 5 (Cy5) bis-NHS-ester dyes using standard protocols as previously described[3]. For each target antigen, multiple clones of primary antibodies were evaluated for sensitivity and specificity. Clones with the best performance characteristics were conjugated, compared with the unconjugated antibody, and then used for multiplex staining. Antibody specificity was evaluated by a clinical pathologist using tissue microarray built for this application including tissue cores from human tonsil, placenta, lung, and liver tissue as well as mouse tissue cores to assess cross-reactivity. The strongest staining and most specific antibodies were further tested to ensure that the antigen was not altered by the dye inactivation process by comparing staining on samples that were untreated or treated 1, 5, or 10 times with the dye inactivation process and subsequent washing in PBS prior to antibody staining.

De-paraffinization, rehydration and antigen retrieval of the FFPE section

Slides were prepared for staining using procedures as described previously.[1] Slides were initially heated for 1 hour at 60°C prior to de-paraffinization with xylene and rehydration through a graded series of ethanol. Two-step antigen retrieval was performed as previously described using

citrate (pH 6) and Tris (pH 9) buffers.[1] Slides were blocked for 1 hour in 4% BSA, 10% donkey serum, in PBS.

Immunofluorescence staining and image acquisition

After blocking, FFPE tissue sections were stained in parallel in the same batch and imaged using the General Electric multiplex fluorescence microscopy platform (INCell Analyzer 2200- https://www.gelifesciences.com/en/us/shop/cell-imaging-and-analysis/high-content-analysis-systems/instruments/in-cell-analyzer-2200-p-00558).[2-4] Each tissue section underwent repeated cycles of staining, imaging, and signal removal. DAPI was used for nuclei image alignment between different rounds of imaging prior to further processing for autofluorescence removal, image segmentation, and quantification of marker expression at single cell level. Image alignment with DAPI minimized the effects of tissue movement and/or tissue loss between staining rounds. Only cells with perfect (100%) alignment with cells in round 0 were included in the analysis. Staining quality was assessed manually as well as semi-automatically. Manual assessment was performed by visualizing staining patterns of individual markers across all samples.

For initial imaging, a 10X objective was used, and the whole tissue was imaged, followed by image stitching to create a composite image of the sample. The large representation of the whole tissue was then converted to a virtual H&E image and used for mapping specific fields for further interrogation of each slide. Slides were then imaged with a 20X objective, dyes inactivated, and re-stained. All dye conjugated antibody stains were incubated for 1 hour at room temperature before slides were processed for staining and washing. Images were captured before

dye inactivation in each cycle. Dye inactivation was performed using an alkaline peroxide solution as previously described[1] and background images were collected between staining rounds to ensure complete inactivation of the fluorochromes. Non-malignant human tonsil, placenta and lung tissues served as positive controls, and mouse (liver, lung and kidney) tissue served as a negative control.

Imaging mass cytometry and immune cell quantification

Archival tissue blocks were used after approval by IRB and written consent from the patient. FFPE tissue sections from biopsy samples were stained in parallel in the same batch, and the Fluidigm Hyperion imaging mass cytometry (IMC) system[5] was used to characterize the TME. The primary interest was to evaluate CD8+ T cells and FOXP3 Tregs based on preliminary data collected through direct immunofluorescence, and other antibodies were used to characterize these primary biomarkers more precisely (Supplemental Table 1).

Preprocessing and Image Acquisition

Laser ablation was used in combination with mass cytometry to enable simultaneous evaluation of multiple biomarkers from tissue sections stained with metal-tagged antibodies. Data acquisition was performed on a Helios time-of-flight mass cytometer (CyTOF) coupled to a Hyperion Imaging System (Fluidigm). The metal composition of the ablated tissue and thus, by inference, the antibody and epitope content was used to create images pixel by pixel, each pixel corresponding to one laser shot.

Cell quantification

Using the automated images generated by the Fluidigm Hyperion IMC system, all tissue regions (not limited to immune "hot spots") were analyzed. The HistoCAT software was used for retrieval of phenotypic and functional marker expression, spatial information, and neighborhood information.[6] Cells were counted in areas of tissue enriched for tumor (>60%). For all analysis, simultaneous visualization of DNA and pan-keratin was performed to verify nuclear and epithelial staining, respectively. For FOXP3 and Ki-67 quantification, positive cells were identified by their characteristic nuclear staining pattern which co-localized with DNA staining[7]. For CD3, CD8 and CD45RO quantification, positive cells were identified by characteristic membranous staining pattern which co-localized with DNA staining.[7] Granzyme B-positive cells were identified by the presence of characteristic intracytoplasmic peripheral granules within CD8-positive cells[7]. All staining patterns were confirmed by comparing with published images.[7] The total tissue area in each section was determined using image analysis software (cellSens).[8] The density of each marker was determined by dividing the total cell count by the total tissue area and expressed as the number of cells per mm^2.

Prior to the main analysis, interobserver variability was determined for two independent observers (L.K., H.Y.) who performed cell quantification of specific markers on gastroesophageal adenocarcinoma FFPE tumor samples according to methodology agreed upon by the two observers and two anatomic pathologists (M.B., R.G.). For FOXP3, correlation coefficient was r =.93 (95% CI 0.80 to 0.98; 15 fields of view). For CD8, correlation coefficient was r =.92 (95% CI 0.82 to 0.97; 20 fields of view). Then for the main analysis, individual cells

were manually counted by a single observer (L.K.) under the direct supervision of an anatomic pathologist (R.G.).

PD-L1 (programmed cell death ligand-1) expression

PD-L1 expression was assessed on FFPE tissue by immunohistochemistry (IHC) (clone 22C3; Dako North America, Carpinteria, CA) with PD-L1-positive defined as a combined positive score (CPS) ≥1. [1,9] The PD-L1 combined positive score (CPS) was calculated using the following formula:

CPS = [Number of PD-L1stained cells (tumor cells, lymphocytes, macrophages) / Total number of viable tumor cells] x 100.

Mismatch repair (MMR) status determination

MMR protein (MLH1, MSH2, PMS2, and MSH6) expression by immunohistochemistry (IHC) was evaluated in FFPE tumor sections in the Division of Anatomic Pathology, Mayo Clinic, as previously described.[10] MMR status was considered deficient (dMMR) if there was loss of expression of one or more MMR proteins and proficient (pMMR) if all MMR proteins were intact.

TABLES

Supplemental Table S1: Antibodies for analysis by Hyperion imaging mass cytometry (IMC).

	Metal Tag	Antibody Clone	Cat#	Dilution
CD8a	162Dy	C8/144B	3162034D	1:100
FoxP3	155Gd	236A/E7	3155016D	1:50
CD3	170Er	Polyclonal	3170019D	1:100
CD4	156Gd	EPR6855	3156033D	1:400
Granzyme B	167Er	EPR20129-217	3167021D	1:50
CD45RO	173Yb	UCHL1	3173016D	1:50
Ki-67	168Er	B56	3168022D	1:50
Pan-Keratin	148Nd	C11	3148020D	1:200
E-Cadherin	158Gd	2.4E+11	3158029D	1:50
DNA	191Ir/193Ir	N/A	N/A	1:400

Supplemental Table S2: Immune checkpoint inhibition agents received.

Agents	**n**
Pembrolizumab	13
Nivolumab	3
Anti-PD-1 antibody + second ICI[a]	2
Anti-PD-1 antibody + antimetabolite ICI[a]	1

[a] Precise identity of agents cannot be disclosed as they were administered as part of a clinical trial which is currently ongoing as of the submission of this manuscript.

Abbreviations: **ICI**, immune checkpoint inhibition; **PD-1**, programmed death-1.

Supplemental Table S3: Last chemotherapy before immunotherapy (n = 17)

Agent(s)	**n**
5-fluorouracil + Oxaliplatin *	14
5-fluorouracil + leucovorin + Irinotecan	1
Docetaxel	1
Ramucirumab	1
None	2

* Thirteen patients received FOLFOX (including with nivolumab [n=2] or trastuzumab [n=1]) and one patient received infusional bolus 5-FU + leucovorin + oxaliplatin once every 2 weeks.

Supplemental Table S4: Best overall response

	ICI-experienced					ICI-naive		
				RAM+TAX with preceding ICI *vs* LCBI [b]			RAM+TAX with *vs* without preceding ICI	
n, number of patients	LCBI (n=17)	ICI (n=19 [a])	RAM+TAX with preceding ICI (n=19 [a])	$P_{unadjusted}$	$P_{adjusted}$	RAM+TAX without preceding ICI (n=68) [c]	$P_{unadjusted}$	$P_{adjusted}$ [d]
Overall response rate (Complete or partial response)	2 (11.8%)	5%	11 (57.9%)	0.003	0.0018	12 (17.7%)	0.0008	< .0001
Complete response	0	0	3 (15.8%)			1 (1.5%)		
Partial response	2 (11.8%)	1 (5.3%)	8 (42.1%)			11 (16.2%)		
Stable disease	7 (41.2%)	2 (10.5%)	4 (21.1%)			16 (23.5%)		
Progressive disease	3 (17.7%)	9 (47.3%)	0			14 (20.6%)		
Not evaluable	5 (29.4%)	7 (37%)	4 (21.1%)			26 (38.2%)		

[a] Includes two patients who received ICI as first-line therapy and thus did not receive LCBI (both patients had progressive disease on ICI, then on subsequent RAM + TAX, one had stable disease and one had partial response). They were appropriately excluded from the comparison of RAM + TAX with preceding ICI *vs* LCBI.

[b] Among patients (n=17) who received both RAM + TAX after ICI and LCBI, best objective response on RAM + TAX after ICI was as follows: complete response (n=3), partial response (n=7), stable disease (n=3), progressive disease (n=0), and non-evaluable (n=4). The overall response rate (complete or partial response) on RAM + TAX after ICI *vs* LCBI was 58.8% (10/17) *vs* 11.8% (2/17) ($P_{unadjusted}$ =.003; $P_{adjusted}$ =.0018 adjusting for ECOG PS).

[c] Forty-two patients were evaluable for response, including one patient who was not evaluable for tumor regression due to lack of measurable disease at baseline, but had progressive disease as best response.

[d] Adjusted for ECOG performance status, age, number of prior lines of therapy, number of metastatic sites, and serum albumin.

Abbreviations: **ICI**; immune checkpoint inhibition; **LCBI**, last chemotherapy before ICI; **RAM+TAX**, ramucirumab/paclitaxel.

Supplemental Table S5: Paired (intrapatient) analyses within the ICI-experienced group comparing clinical outcomes during ramucirumab/paclitaxel after ICI *vs* during the last chemotherapy before ICI in patients evaluable during both treatment segments.

Clinical outcome variable	No. pairs	Ramucirumab/paclitaxel with preceding ICI [a]		Last chemotherapy before ICI [a]		Difference		*P* [c]
		Median (Mean)	95% CI	Median (Mean)	95% CI	Median (Mean)	95% CI	
Tumor regression, %	9	-50.0% (-56.4%)	-84.0% to -28.9% [b]	7.1% (5.3%)	-17.5% to 28.0% [b]	-67.6% (-61.7%)	-103.2% to -20.2% [b]	0.019
Progression-free survival, months	17 [d]	12.2	6.4 to 12.6	3.0	1.8 to 5.1	4.0 (5.2)	1.4 – 9.0 [b]	0.0027
	7 [e]	8.9	3.4 to 12.5	1.8	1.1 to 6.1	6.1 (5.8)	3.3 – 8.2 [b]	0.016

[a] Values are meant only for description to characterize the distribution within a group (they are not the precise components utilized in paired calculations). Paired calculations were performed intrapatient.

[b] 95% CI refers to mean.

[c] Wilcoxon signed rank

[d] All patients regardless of whether a PFS event occurred

[e] All patients who had a PFS event during both segments of therapy. Appropriately excludes 10 patients (3 patients discontinued the last chemotherapy before ICI due to toxicity without a PFS event, 7 other patients received ramucirumab/paclitaxel after ICI and have not had a PFS event).

Abbreviations: **ICI**; immune checkpoint inhibition; **CI**; confidence interval; **PFS,** progression-free survival

Supplemental Table S6: Outcomes on ramucirumab/paclitaxel as reported in literature.

	Phase 3 trial RAINBOW (Region 1-2 [outside of Asia]) [11]	**"Real-world" RAMoss (Italian)** [12]	**"Real-world" KCSG (Korean)** [13]	**Current study (ICI-naïve)**
ORR	25% *	20.2% *	16.6% *	17.7% (95% CI 10.4, 28.4)
mPFS	4.2 m (95% CI 3.9, 4.9)	4.5 m (95% CI 4.1–4.8)	3.8 m (95% CI 3.4, 4.4)	4.9 m (95% CI 3.7, 6.0)
mOS	8.5 m (95% CI 7.4, 9.8]	8.3 m (95% CI 7.2, 8.8)	8.6 m (95% CI 7.7, 10.0)	7.4 m (95% CI 6.1, 10.1)
* 95% CI not reported				

Abbreviations: **ICI**, immune checkpoint inhibition; **mOS**, median overall survival; **mPFS**, median progression-free survival; **ORR**, overall response rate.

FIGURES

Supplemental Figure S1: **CONSORT DIAGRAM**

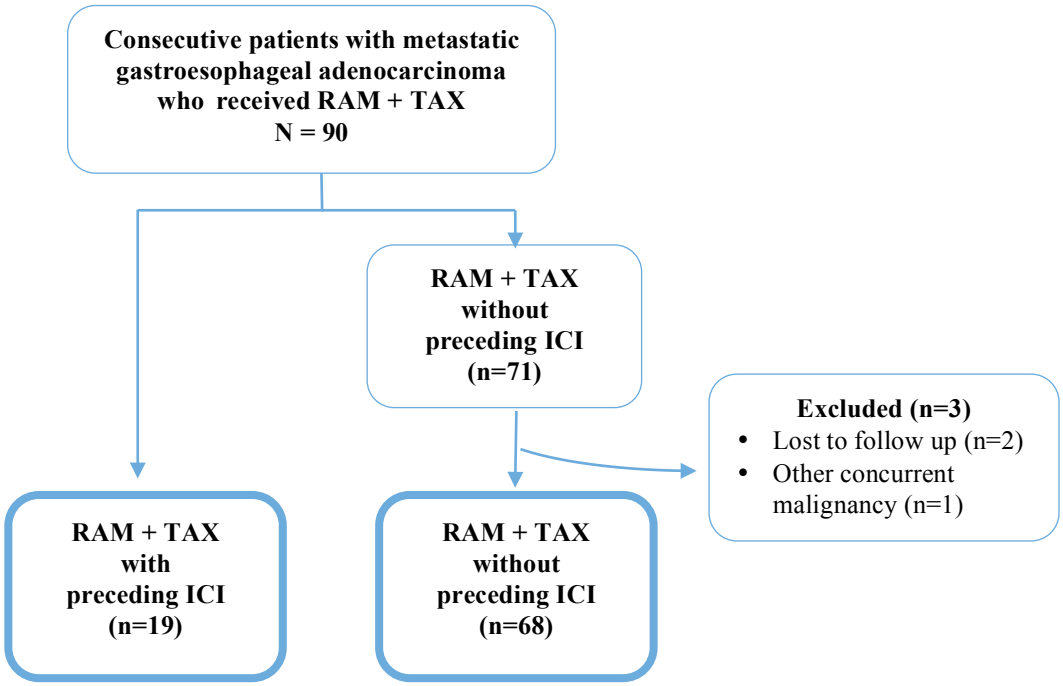

Abbreviations: **ICI**, Immune checkpoint inhibition; **RAM**, ramucirumab; **TAX**, paclitaxel.

Supplemental Figure S2. Representative serial radiographic images of patient responders.

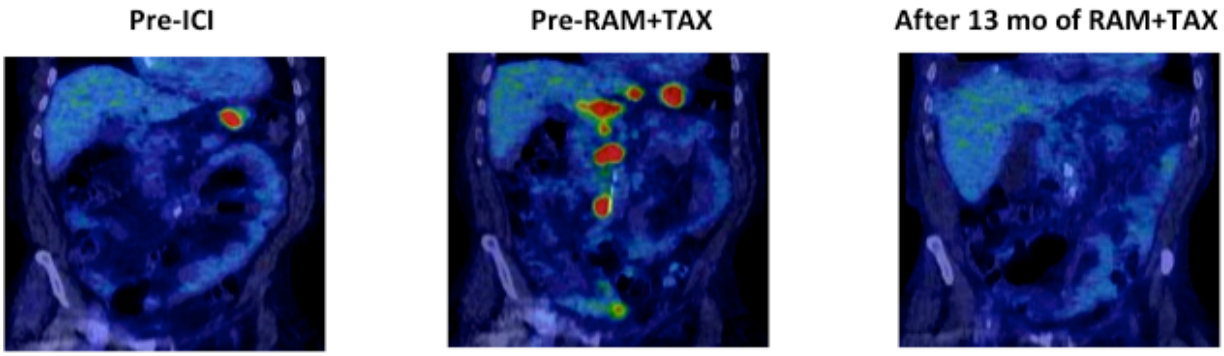

(A) ^{18}F-fluoro-deoxyglucose Positron Emission Tomography/Computed Tomography (PET/CT) images showing uptake in the primary tumor, pre-ICI, with a best response of progression on ICI to involve lymph nodes (portohepatic, gastrohepatic, retroperitoneal) and hepatic metastases, and with complete response on subsequent ramucirumab/paclitaxel.

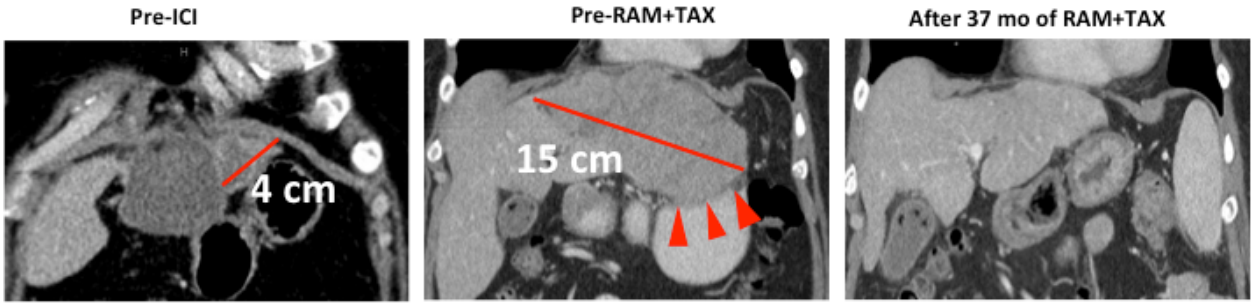

(B) Contrast-enhanced computed tomography images showing a liver metastasis adjacent to an ablation defect. ICI led to a best response of progression, with symptomatic infiltration of the liver metastasis into adjacent stomach (arrowheads), followed by durable complete response on subsequent ramucirumab/paclitaxel.

Abbreviations: **ICI**, Immune checkpoint inhibition; **RAM**, ramucirumab; **TAX**, paclitaxel.

Supplemental Figure S3. Swimmer plot of ramucirumab/paclitaxel in ICI-experienced patients (n=19 patients). Shown are the duration of ramucirumab/paclitaxel after irRECIST progression on ICI, clinical response per RECIST1.1, and PD-L1 and MMR status in patient tumors. Repulsing with ICI refers to re-exposure to one dose of anti-PD-1 therapy followed by one cycle of ramucirumab/paclitaxel, repeated until progression or intolerance. Response duration was conservatively censored at the time of re-pulsing.

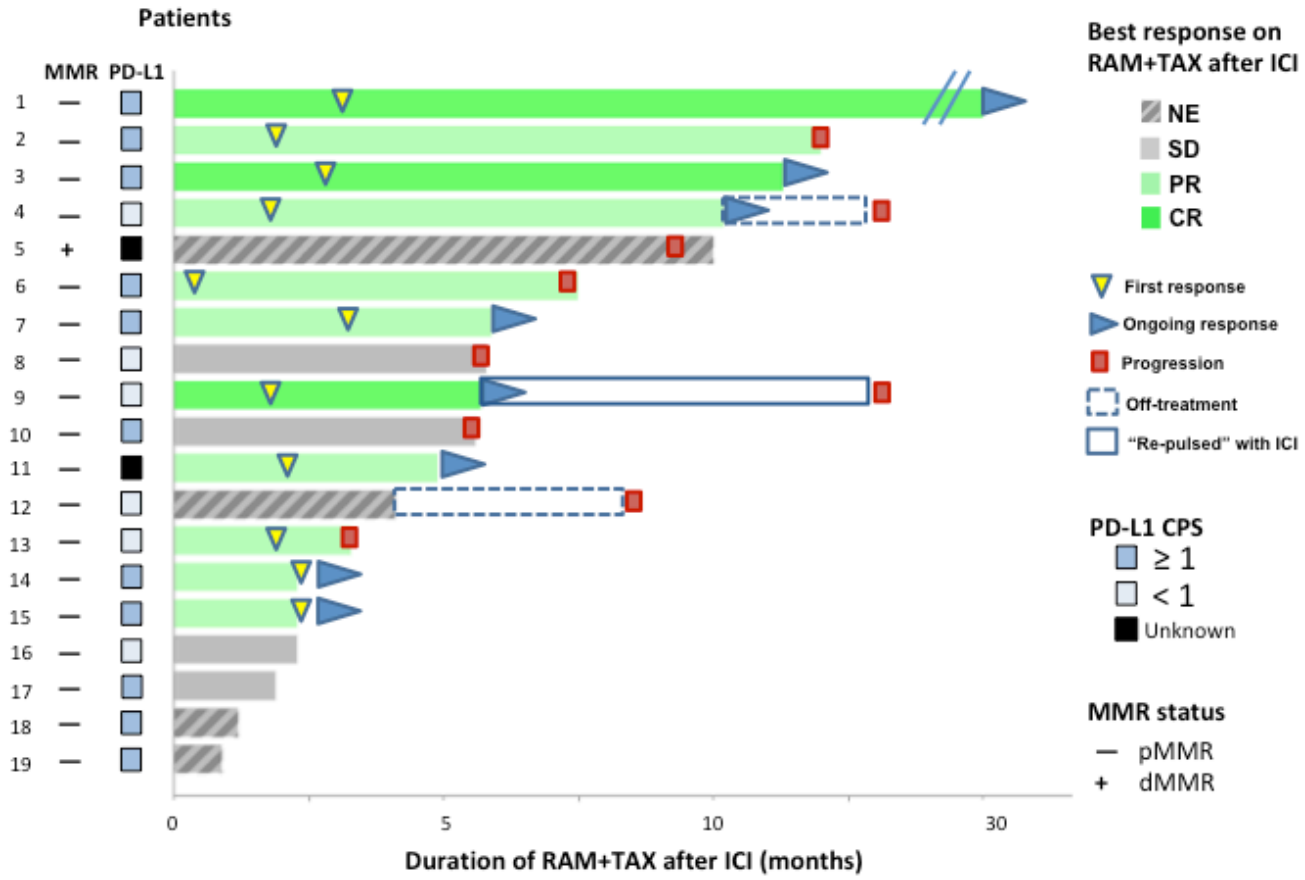

Abbreviations: **ICI**, Immune checkpoint inhibition; **RAM**, ramucirumab; **TAX**, paclitaxel; **PD-L1**, programmed death-ligand 1; **CPS**, combined positive score; **pMMR**, proficient mismatch repair; **dMMR**, deficient mismatch repair.

Supplemental Figure S4: **Paired (intrapatient) analysis of best response per RECISTv1.1 during the last chemotherapy before ICI *vs* during ramucirumab/paclitaxel immediately after ICI in patients evaluable for response during both segments of therapy (n = 9 patients).** The color of arrows denotes improved (green), same (gray), or worsened (red) response category during ramucirumab/paclitaxel as compared with during the last chemotherapy before ICI. * *P* =.034 McNemar's test for paired data grouping SD with PD and PR with CR.

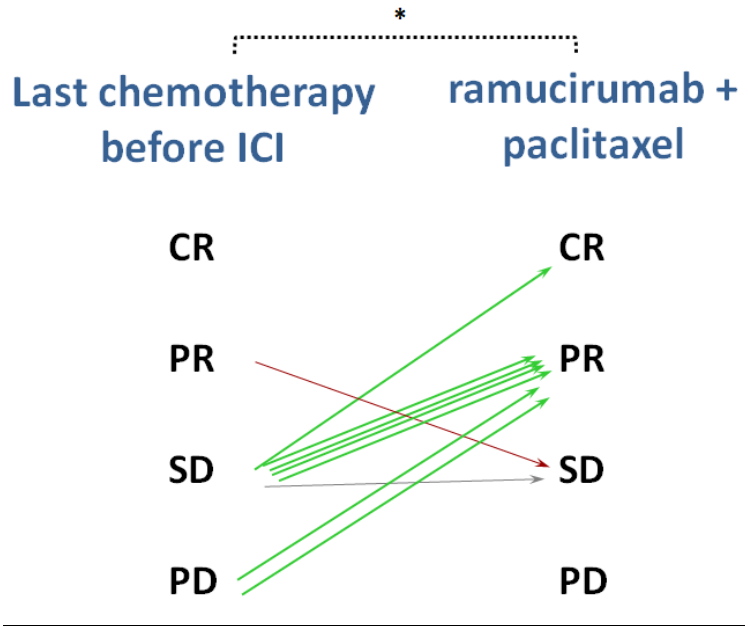

Abbreviations: **ICI**, Immune checkpoint inhibition; **RAM**, ramucirumab; **TAX**, paclitaxel; **LCBI**, last chemotherapy before ICI; **CR**, complete response; **PR**, partial response; **SD**, stable disease; **PD**, progressive disease.

Supplemental Figure S5: **Baseline host and tumor characteristics in ICI-naïve and ICI-experienced patients immediately prior to administration of ramucirumab/paclitaxel (N = 87).** Each row represents a unique patient. Gray cells denote missing data or not applicable, as appropriate.

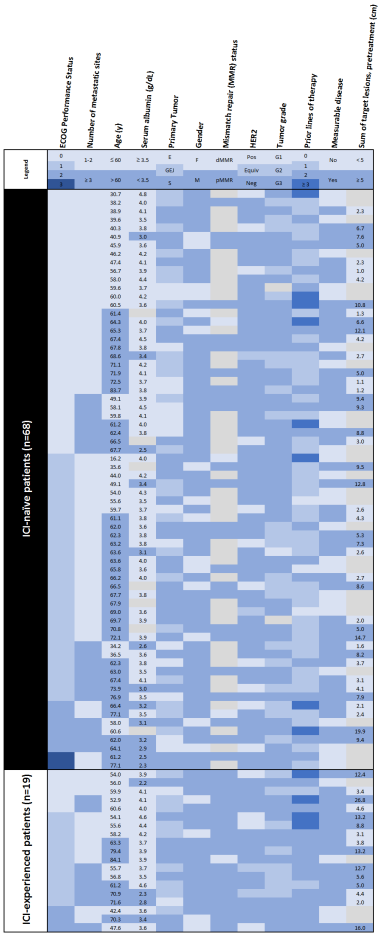

Abbreviations: **ICI**, Immune checkpoint inhibition.

REFERENCES

1. Gerdes MJ, Sevinsky CJ, Sood A, et al. Highly multiplexed single-cell analysis of formalin-fixed, paraffin-embedded cancer tissue. *Proc Natl Acad Sci* USA. 2013;110(29):11982-11987. doi:10.1073/pnas.1300136110

2. Gerdes MJ, Gökmen-Polar Y, Sui Y, et al. Single-cell heterogeneity in ductal carcinoma in situ of breast. *Mod Pathol*. 2018;31(3):406-417. doi:10.1038/modpathol.2017.143

3. McKinley ET, Sui Y, Al-Kofahi Y, et al. Optimized multiplex immunofluorescence single-cell analysis reveals tuft cell heterogeneity. *JCI Insight*. 2017;2(11):e93487. Published 2017 Jun 2. doi:10.1172/jci.insight.93487

4. Sood A, Miller AM, Brogi E, et al. Multiplexed immunofluorescence delineates proteomic cancer cell states associated with metabolism. *JCI Insight*. 2016;1(6):e87030. doi:10.1172/jci.insight.87030

5. Jackson HW, Fischer JR, Zanotelli VR, et al. The single-cell pathology landscape of breast cancer. *Nature*. 2020 Feb;578(7796):615-20.

6. Schapiro D, Jackson HW, Raghuraman S, et al. histoCAT: analysis of cell phenotypes and interactions in multiplex image cytometry data. *Nat Methods*. 2017;14(9):873-876. doi:10.1038/nmeth.4391

7. Parra ER, Uraoka N, Jiang M, et al. Validation of multiplex immunofluorescence panels using multispectral microscopy for immune-profiling of formalin-fixed and paraffin-embedded human tumor tissues. *Sci Rep*. 2017;7(1):13380. doi:10.1038/s41598-017-13942-8

8. Bois MC, May AM, Vassallo R, Jenkins SM, Yi ES, Roden AC. Morphometric Study of Pulmonary Arterial Changes in Pulmonary Langerhans Cell Histiocytosis. *Arch Pathol Lab Med*. 2018;142(8):929-937. doi:10.5858/arpa.2017-0463-OA

9. Kulangara K, Zhang N, Corigliano E, et al. Clinical Utility of the Combined Positive Score for Programmed Death Ligand-1 Expression and the Approval of Pembrolizumab for Treatment of Gastric Cancer. Arch Pathol Lab Med. 2019;143(3):330-337. doi:10.5858/arpa.2018-0043-OA

10. Sinicrope FA, Mahoney MR, Smyrk TC, et al. Prognostic impact of deficient DNA mismatch repair in patients with stage III colon cancer from a randomized trial of FOLFOX-based adjuvant chemotherapy. *J Clin Oncol*. 2013;31(29):3664-3672. doi:10.1200/JCO.2013.48.9591

11. Wilke H, Muro K, Van Cutsem E, et al. Ramucirumab plus paclitaxel versus placebo plus paclitaxel in patients with previously treated advanced gastric or gastro-oesophageal junction adenocarcinoma (RAINBOW): a double-blind, randomised phase 3 trial. *Lancet Oncol.* 2014;15(11):1224-1235. doi:10.1016/S1470-2045(14)70420-6

12. Di Bartolomeo M, Niger M, Tirino G, et al. Ramucirumab as Second-Line Therapy in Metastatic Gastric Cancer: Real-World Data from the RAMoss Study. *Target Oncol*. 2018;13(2):227-234. doi:10.1007/s11523-018-0562-5

13. Jung M, Ryu MH, Oh DY, et al. Efficacy and tolerability of ramucirumab monotherapy or in combination with paclitaxel in gastric cancer patients from the Expanded Access Program Cohort by the Korean Cancer Study Group (KCSG). *Gastric Cancer*. 2018;21(5):819-830. doi:10.1007/s10120-018-0806-1